eNeuro

Research Article: New Research | Sensory and Motor Systems

Taste-odor association learning alters the dynamics of intra-oral odor responses in the posterior piriform cortex of awake rats

https://doi.org/10.1523/ENEURO.0010-23.2023

Cite as: eNeuro 2023; 10.1523/ENEURO.0010-23.2023

Received: 6 January 2023
Revised: 14 February 2023
Accepted: 23 February 2023

Taste-odor association learning alters the dynamics of intra-oral odor responses in the posterior piriform cortex of awake rats

Joost X. Maier, Ammar Idris & Brooke A. Christensen

Department of Neurobiology & Anatomy, Wake Forest Atrium Baptist Medical Center, Winston-Salem, NC

Abbreviated title: Learning-related neural activity in olfactory cortex

Number of Figures: 7

Number of words: 245 (Abstract); 778 (Introduction); 1760 (Discussion)

*Correspondence:

Joost X. Maier

Wake Forest School of Medicine

Department of Neurobiology & Anatomy

Medical Center Blvd

Winston-Salem, NC 27157

USA

Email: jmaier@wakehealth.edu

Phone: +1 336-713-4760

Acknowledgements

Many thanks to Chad Collins for excellent technical assistance, and to Ellen Walker for help with data collection.

Competing Interest Statement

The authors declare that they have no competing interests.

Funding Sources

This work is supported by NIH R01 DC016063.

Abstract

How an odor is perceived is to a large extent dependent on the context in which that odor is (or has been) experienced. For example, experiencing an odor in mixture with taste during consumption can instill taste qualities in the percept of that odor (e.g., vanilla—an odor—has a gustatory quality: sweet). How associative features of odors are encoded in the brain remains unknown, but previous work suggests an important role for ongoing interactions between piriform cortex and extra-olfactory systems. Here we tested the hypothesis that piriform cortex dynamically encodes taste associations of odors. Rats were trained to associate one of two odors with saccharin; the other odor remained neutral. Before and after training, we tested preferences for the saccharin-associated odor versus the neutral odor, and recorded spiking responses from ensembles of neurons in posterior piriform cortex (pPC) to intra-oral delivery of small drops of the same odor solutions. The results show that animals successfully learned taste-odor associations. At the neural level, single pPC neuron responses to the saccharin-paired odor were selectively altered following conditioning. Altered response patterns appeared after 1 second following stimulus delivery, and successfully discriminated between the two odors. However, firing rate patterns in the late epoch appeared different from firing rates early in the early epoch (<1 second following stimulus delivery). That is, in different response epoch, neurons used different codes to represent the difference between the two odors. The same dynamic coding scheme was observed at the ensemble level.

Significance Statement

Odors carry important meaning beyond their chemical identity. One particularly salient example of this are food odors, which play an important role in determining flavor preferences and food choice behavior. How these extra-olfactory aspects of odor are represented is unknown. Using extracellular recordings in awake rats in the context of a flavor preference learning task, we show that learned taste associations of odor stimuli are represented in the dynamic firing patterns of posterior piriform cortex neurons. The results suggest that associative odor coding results from ongoing interactions between olfactory and extra-olfactory systems.

Introduction

Smell is unique among the senses in that it faces an extraordinary large number of potential sensory qualities (Bushdid et al., 2014). To meet this challenge, olfactory space is not represented in fixed, topographically organized maps as in other sensory systems (Rennaker et al., 2007; Stettler and Axel, 2009). Instead, cortical odor coding is highly plastic and depends to a large extent on the context in which an individual experiences an odor (Wilson and Stevenson, 2003; Wilson et al., 2004).

One particularly salient context in which olfaction plays a major role is consumption. During consumption, odor stimuli are typically experienced in mixture with taste. Behavioral work has shown that interactions between taste and odor components of flavor are highly adaptive in informing consumption decisions (Holman, 1975; Sclafani and Ackroff, 1994; Slotnick et al., 1997; Blankenship et al., 2019; Elliott and Maier, 2020; Maier and Elliott, 2020). One example of taste-odor interactions during consumption is the formation of taste-odor associations. Odors experienced in mixture with taste acquire qualities associated with that taste (Stevenson et al., 1995; Stevenson et al., 1998; Stevenson et al., 2000a; Stevenson et al., 2000b; Stevenson and Boakes, 2004; Yeomans et al., 2006; McQueen et al., 2020). Taste-odor association learning is robust, rapid, and affects subsequent consumption behavior: odors that have been experienced in mixture with palatable tastes become attractive.

Recent work aimed at elucidating how taste-odor associations are represented in the brain has indicated a role for the insular gustatory cortex (GC). Optogenetic inhibition of GC after rats learned to associate an odor with saccharin (a sweet taste) impaired their ability to express a preference for that odor (Maier et al., 2015; Blankenship et al., 2019). However, how GC exerts its effect on neural coding of taste-odor associations is unknown. Taste-odor associations may reside locally in GC. Alternatively, GC may support taste-odor associations by modulating sensory processing in olfactory areas. One potential area through which GC may affect olfactory processing is the piriform (olfactory) cortex—a large cortical surface that receives bottom-up input from the olfactory bulb representing a vast space of odorant molecules (Scott et al., 1980; Schwob and Price, 1984; Rennaker et al., 2007; Stettler and Axel, 2009; Miyamichi et al., 2011; Sosulski et al., 2011). Moreover, the piriform cortex is ideally

situated to interact with extra-olfactory systems (Luskin and Price, 1983; Johnson et al., 2000; Haberly, 2001; Majak et al., 2004; Sadrian and Wilson, 2015), sculpting odor representations based on the context an odor is encountered in (Kadohisa and Wilson, 2006; Li et al., 2006; Calu et al., 2007; Roesch et al., 2007; Li et al., 2008; Barnes et al., 2011; Chen et al., 2011; Chapuis and Wilson, 2012; Gire et al., 2013; Meissner-Bernard et al., 2019; Wang et al., 2019). Interactions with extra-olfactory systems are particularly pronounced in the posterior piriform cortex (pPC) (Johnson et al., 2000; Majak et al., 2004; Zelano et al., 2005; Li et al., 2006; Calu et al., 2007). Indeed, pPC odor representations have been shown to be affected by experience and multisensory context (Karunanayaka et al., 2015; Avery et al., 2020). Previous work from our lab identified GC as a source of extra-olfactory input to pPC, as inactivation of GC affects pPC responses to taste stimuli, as well as odor stimuli even in the absence of concurrent taste input (Maier et al., 2015). Together, these findings suggest that encoding of taste-odor associations may be supported by ongoing interactions between GC and pPC.

Here, we test the hypothesis that taste associations of odor stimuli are represented in pPC. Specifically, we predict that experience with taste-smell mixtures affects responses of pPC neurons to intraoral delivery of odor solutions. We further predict that the effect of experience is reflected in changes in response dynamics, consistent with the idea that odor coding in the context of consumption depends on ongoing interactions with the taste system. Alternatively, if taste associations are represented locally in GC, we do not predict any experience-dependent changes in responsiveness at the level of pPC. Associations may also be represented locally in pPC, independently of GC. In this case, we expect experience to be reflected in static pPC response patterns. To test our predictions regarding neural coding of taste-odor associations, we used extracellular electrophysiology to record spiking activity from ensembles of single pPC neurons of awake rats while they consumed odor solutions, before and after taste-odor association learning. We show that taste-odor association learning changes the temporal dynamics of odor responses, such that initial odor-selective response patterns are transformed over the course of seconds into a novel representation that distinguishes taste-associated from taste-naïve odors. These results suggest that pPC dynamically encodes both odor identity and taste association.

Methods

Subjects

A total of 30 adult female Long-Evans rats (www.criver.com), weighing between 250 and 300 g at the time of surgery served as subjects. All rats were individually housed and kept on a 12/12 hour light/dark cycle (ZT0=06:00). Experiments were conducted during the light cycle. All animal procedures were performed in accordance with the Wake Forest Atrium Baptist Medical Center animal care committee's regulations.

Surgery

Animals were injected intraperitoneally with the analgesic meloxicam (10 mg/kg) prior to surgery. Stereotaxic surgery was performed under intranasally administered isoflurane anesthesia (2-5%). First, the scalp was treated with lidocaine ointment, an incision was made, and the skin retracted from the skull. Using a dental drill, a craniotomy was made overlying the posterior piriform olfactory cortex (uni- or bilateral): 1.4 mm posterior to bregma, 5.2-5.6 mm lateral to the midline, 6.4-7.4 mm ventral from the surface of the brain (Paxinos and Watson, 1986). Five additional burr holes were made, evenly spread across the skull, for the insertion of skull screws that provide stability to the implant. Electrodes were then lowered to the piriform cortex over the course of 30 minutes using a manually-driven stereotaxic arm. Once in place, the craniotomy was filled with Kwik-Cast (www.wpiinc.com), and the electrode connector and skull screws were covered in dental acrylic, fixing the electrodes in place. Electrode assemblies consisted of micro-wire arrays with 6 or 8 electrodes in circular arrangement, or 16 electrodes in square arrangement. Electrodes were 25 µm diameter stainless steel wires, spaced 100-200 µm apart (www.microprobes.com), or multi-electrode silicon probes (2 shanks of 16 electrode contacts each, shanks spaced 500 µm apart; electrode contacts spaced 50 µm apart, www.neuronexus.com model A2x16-10mm-50-500-177-CM32). Intra-oral cannulae (IOC) were implanted to provide access to the oral cavity (Phillips and Norgren, 1970): Flanged microbore PE tubing (1.143 mm ID, 1.574 mm OD) was inserted behind the second molar using a 20 G needle, and guided under the skin overlying the zygomatic arch to exit at the edge of the cranial implant. Tubing was then attached to a coupler body (www.cpcworldwide.com, #SMF01) that could interface with a counterpart holding a manifold of fluid delivery tubes. Once in place, the

coupler was secured to the rest of the implant with dental acrylic. Animals recovered in their home cage with *ad lib* access to water and mashed rat chow for 4-5 days after surgery before the start of the experiment.

Stimuli

Unisensory odor stimuli were exemplars of monomolecular odorants (obtained from www.sigmaaldrich.com), >98% purity) that have been used in similar behavioral (Blankenship et al., 2019) and neural recording (Maier, 2017) paradigms in previous studies: methyl valerate and 2-hexanone in aqueous solution (0.025% volume/volume in distilled water). Saccharin (0.2%; www.fishersci.com) was used as an unconditioned stimulus during conditioning sessions. All stimuli were presented intra-orally in order to allow—as much as possible—natural sensory stimulation dynamics associated with intra-oral evaluation of flavor. There is no empirical evidence that the odorants used here completely lack gustatory and/or trigeminal qualities. However, similar concentrations of odor solutions have been shown to be below non-olfactory behavioral detection thresholds (Slotnick et al., 1997; Gautam and Verhagen, 2012), and are therefore unlikely to have contributed to the observed responses.

Behavioral procedures

Preference testing: Two-bottle tests were used to assess odor preferences before and after conditioning. During each preference testing session, animals were given free access to two odor solutions overnight (18:00 – 08:00). Animals received *ad lib* access to water in between two-bottle tests, ensuring that they were never deprived of fluid during preference testing sessions. Relative position of the odor bottles in the cage was alternated between sessions and counterbalanced across rats. In one preference test, consumption from one bottle could not be determined due to spillage (0.8% of all bottles); data from this animal was excluded from contributing to the behavioral dataset. *Conditioning:* One-bottle access was used for conditioning, performed over 4 consecutive days. Each morning (10 AM), animals had access to 10 ml of one of the odors (odor A) in plain water, or the other odor (odor B) in saccharin solution for 30 minutes. Bottles alternated on an A-B-A-B schedule, and the identity of odors A and B (methyl valerate or 2-hexanone) was counterbalanced across rats.

Stimulus presentation and recording procedures

The recording arena consisted of a 29×23×33 cm Plexiglas chamber encased in metal that served as a Faraday cage. Stimuli were delivered via syringe pumps directly onto the dorsal surface of the tongue while animals were moving freely around the arena. Syringes containing stimulus solution were connected to blunted needles fitted with strands of PE tubing (1.143 mm ID, 1.574 mm OD) that fed into the recording arena via an opening in the roof. At the distal end of each strand of PE tubing, a 5 cm strand of PI microbore tubing (0.0254 mm ID, 0.0270 mm OD) was glued, and all tubes were inserted into the through hole of a coupler body (www.cpcworldwide.com, #SMF02) and held together with glue. Before experimental sessions, the collection of PI tubes was fed into the IOC and secured in place by mating the coupler bodies on the tube manifold and IOC. Once connected, the tips of the PI tubes extended 0.5 mm below the tip of the IOC into the oral cavity. Animals were habituated to the recording setup and stimulus delivery apparatus prior to recording by presenting drops of water through IOC in the recording arena. During recording sessions, airborne odorants were cleared by a continuously running fan mounted in the ceiling of the recording arena. To encourage consumption of stimuli, animals were deprived of water for 6 hours before recording sessions. During each recording session, odors A and B, as well as plain water were presented in random order (10 repetitions of each stimulus). Stimuli were always presented in random order. Intra-oral stimuli were delivered in 30-50 µl aliquots (total duration of delivery <100 ms), with a random inter-trial interval ranging from 30-45 s, allowing sufficient time for animals to swallow the fluid and clear their mouth. Each session yielded between 1 and 16 (mean=5.0) single neurons (0.3 neurons/electrode on average). In a subset of animals, multisensory mixtures of odors A/B and taste compounds (saccharin and/or sodium chloride), as well as unisensory taste compounds in isolation, were presented in addition to the stimuli listed above (data not included in the present paper). During these sessions, both odorants were paired with the same tastant(s) for 10 trials per mixture. Recording and preference testing sessions were always performed according to the schedule listed in Figure 2. Given the limited and balanced nature of mixture exposure during recording sessions, it is unlikely to have impacted the results reported in the present study. Results from a subset of recordings in response to mixtures have been reported previously (Idris et al., 2023).

Electrophysiological recording and data processing

The continuous extracellular signal recorded from each electrode was amplified, digitized and stored for offline analysis at a sampling rate of 25 kHz using INTAN RHD2000 hardware and acquisition software (www.intantech.com). Action potentials were extracted, clustered and sorted using the klusta/phy toolbox to obtain single neuron spike time stamps (Rossant et al., 2016). For silicon probe recordings, spikes were clustered taking into account the possibility that the same action potentials could be recorded by up to three neighboring channels. Spike time stamps were then binned at 1 ms resolution and aligned to stimulus delivery before further analysis. Only action potentials that exceeded 3.5 standard deviation units of the high-pass filtered (400 Hz) voltage signal were included in the clustering analysis, and only clusters that contained less than 2% of action potentials occurring at an inter-spike interval of 2 ms or less were included in the dataset (Gadziola et al., 2015).

Data analysis

Offline analyses were performed using Matlab (www.mathworks.com). For time-averaged analysis, responses were averaged over the following time windows relative to stimulus delivery: −2000-0 ms (baseline period), 0-2500 ms (total stimulus period), 0-1250 ms (early stimulus period), 1250-2500 ms (late stimulus period). For time-resolved analysis, responses were averaged in a sliding window over time (window size: 500 ms; step size: 50 ms). Cohen's d was calculated to provide a continuous measure of effect size (discriminability) for each neuron: Cohen's $d=(mean_A-mean_B)/std_{pooled}$, where $std_{pooled}=([std_A^2+std_B^2])/2$.

To make the connection between firing rates of individual neurons and the amount of information present in the collective responses of ensembles of neurons, we performed single-trial ensemble decoding analysis (Quiroga et al., 2007; Bolding and Franks, 2017). Specifically, we asked how well odors A and B could be discriminated based on the firing rates of all simultaneously-recorded single neurons during a given session. For each temporal analysis window (i.e., baseline, stimulus, sliding window over time), we first computed single-trial ensemble response vectors, consisting of the time-averaged response in that window for each simultaneously-recorded neuron. Each single-trial ensemble response vector was then compared to two templates (A and B), consisting of the ensemble response vectors averaged

across all odor A and odor B trials (excluding the trial to be decoded). Similarity of each trial to both templates was then quantified by calculating the Euclidean distance. Decoding accuracy was defined as the percentage of trials that showed greater similarity with the correct template (i.e., an ensemble response on an odor A trial showing higher similarity with the odor A template than with the odor B template, and vice versa).

Histology

Electrodes were labeled with a drop of Vybrant® DiI cell-labeling solution (www.thermofisher.com), applied with a needle tip before implantation, allowing *post mortem* reconstruction of the implant location. In order to do so, rats were perfused trans-cardially with saline and 10% formalin, their brains extracted and placed in 30% sucrose for 3-5 days. Brains were then frozen; coronal sections were cut around the implant location using a sliding microtome, mounted on glass slides in DAPI Fluoromount-G medium (www.southernbiotech.com) and a cover-slip was applied. Epifluorescence microscopy was used to visualize DiI and DAPI. Figure 1 shows histological reconstruction of electrode placement in pPC for two representative animals.

Statistics

Statistical tests involved comparing distributions of quantities (preference, firing rate, effect size, decoding accuracy) over animals, trials, neurons or sessions These distributions followed approximately normal distributions. Repeated measures (i.e., preference pre and post conditioning, activity during stimulus and baseline periods) were compared using a paired samples t-test. Other comparisons were performed using an independent samples t-test. Similarly, factors in analysis of variance (ANOVA) were treated as within- or between-subjects as applicable. Frequency of occurrence was compared between conditions using non-parametric sign-test or chi-square test. All tests were two-tailed with α=0.05.

Results

Behavioral assessment of taste-odor association learning

The present study aimed to elucidate the neural representation of taste-odor associations. In particular, we tested the hypothesis that taste associations of odors are encoded in the activity of pPC neurons via ongoing top-down modulations. Odor-taste association learning was established and assessed using a two-bottle consumption task in which we measured relative preference for a test odor B versus a control odor A, before and after animals learned to associate odor B with 0.2% saccharin (a palatable sweet taste). An outline of the experimental protocol is shown in Figure 2A. Figure 2B shows preferences for odor B (relative to odor A) before and after conditioning. After conditioning, a significant majority of animals (23 out of 29, 79%, sign test: $p<0.01$) increased their preference for the saccharin-paired odor (Figure 2C; t-test comparing preferences before and after conditioning: $t_{28}=2.94$, $p<0.01$). Thus, our training procedure was effective in conditioning a preference for the saccharin-paired odor relative to the control odor, consistent with previous work (Holman, 1975; Maier et al., 2015; Blankenship et al., 2019; Christensen et al., 2022).

Responsiveness of single pPC neurons to odor solutions

To investigate how neurons in pPC may encode taste-odor associations, we recorded responses from small ensembles of single pPC neurons to intra-oral delivery of odor A and B solutions before and after preference learning. Stimuli were presented intra-orally to allow—as much as possible—the natural dynamics of sensory stimulation that occurs during oral evaluation of flavor, including retronasal odorant delivery, concurrent somatosensory stimulation and orofacial behaviors associated with consumption. A total of 299 single neurons were isolated across the two recording sessions per animal (n=152 and 147 neurons before and after conditioning, respectively). Figure 3 shows examples of single pPC neuron responses, highlighting the main patterns observed across the population. The neurons in panels A-B were recorded before conditioning; the neurons in panels C-D were recorded after conditioning. Responses were often odor-selective (e.g., Figure 3A, C-D, where responses differed between odors A and B as determined by independent samples t-test comparing average responses in stimulus period [2.5 s window immediately following stimulus onset]); responses typically

283 exhibited sustained responses across the stimulus period; and could be excited (Figure 3A, C) or
284 inhibited (Figure 3B) relative to baseline (as determined by paired samples t-test comparing
285 average responses in the stimulus period versus baseline [2.5 seconds immediately preceding
286 stimulus onset]). Some responses appeared to exhibit complex dynamics. For example, the
287 response to odor B for the neuron shown in Figure 3D switched from being inhibited early in
288 the response to being excited later in the response. In order to determine how pPC neurons
289 may represent information about the odor stimuli, we first quantified the number of neurons
290 that respond to each odor. Given the variable and protracted response dynamics observed in
291 individual neuron response profiles (see Figure 3), we performed a sliding window analysis,
292 comparing responses in overlapping 500 ms bins to baseline using a paired samples t-test.
293 Figure 4A-B shows the number of neurons that responded significantly to odors A and B as a
294 function of time following stimulus delivery. Overall, each odor evoked sparse responses in pPC
295 (up to 20% of total neurons at any point in time during the stimulus period), in line with
296 previous work using orthonasal as well as retronasal odorants. The number of neurons did not
297 differ between odors, or between pre and post conditioning (X^2 test: $p>0.05$ for all time
298 windows).
299 *Dynamics of odor-selectivity in single pPC neurons changes after conditioning*
300 The example responses shown in Figure 3 demonstrate that single pPC neuron responses can
301 respond to multiple odors in a more or less selective manner. This pattern is generally in line
302 with previous work using orthonasal odorants showing that different odors elicit responses in
303 partly overlapping ensembles of piriform cortex neurons. To determine how well individual
304 neurons distinguish between odors A and B, we analyzed neurons that exhibited significant
305 overall responsiveness, defined as a significant response to odor (pooled across odors A and B)
306 in the stimulus period versus baseline (n=36 neurons before and after conditioning). Cohen's d
307 was used as a continuous measure of discriminability. We calculated discriminability in two
308 time windows (0-1250 and 1250-2500 ms following stimulus delivery). Figure 5A shows average
309 discriminability before and after conditioning during the early and late time windows, as well as
310 during the baseline period. Two-way ANOVA on the magnitude of discriminability (i.e., the
311 absolute value of Cohen's d) with factors Window (early, late) and Epoch (pre, post) revealed a

significant Window × Epoch interaction ($F_{1,279}$=4.48, p<0.05). Post-hoc comparisons (Bonferroni corrected) indicated that discriminability was significantly increased during the early portion of the response relative to baseline, and that during the late portion of the response, discriminability was significantly higher post versus pre conditioning. The increase in discriminability late in the response observed after conditioning could be the result of two scenarios. First, individual neurons could sustain their activity patterns established early in response (e.g., the neuron shown in Figure 3C that prefers odor B over A during both the early and late portion of the response). Alternatively, activity patterns could differ between the early and late portion of the response (e.g., the neuron shown in Figure 3D that is non-selectively early in the response, followed by an increase in firing rate in response to odor B over A later in the response). In the first scenario, raw Cohen's d values obtained from the two response windows would be highly correlated. That is, the early and late portions of the response should exhibit similar odor selectivity. In the second scenario, raw Cohen's d values obtained from the two response windows may be unrelated or even anti-correlated. Figure 5B shows raw Cohen's d values obtained from the two response windows for all stimulus responsive neurons recorded pre and post conditioning. Pre conditioning, odor discriminability is highly correlated between the two response windows (r=0.68, p<0.001), suggesting that odor selectivity established early in the response is to some extent sustained during the late portion of the response. Post conditioning, correlation between the two response windows is significantly reduced (F-test comparing correlations obtained pre and post conditioning: z=1.78, p<0.05), despite the fact that discriminability is significant in the late portion of the response, and is—if anything—increased relative to the early portion of the response. This pattern of results is consistent with the second scenario, in which odor-evoked responses undergo pronounced qualitative changes over the course of the response post conditioning. Thus, odor-taste conditioning is associated with changes in the pattern of responses during the late epoch, such that odor discriminability is increased.

Odor information is present in single trial pPC ensemble responses

The analyses described above assessed responsiveness and discriminability of odors A and B at the level of single pPC neurons that were selected based on arbitrary response properties (i.e.,

significant responsiveness versus baseline). However, across the population of animals, few neurons exhibited significant responses, and the analysis presented above thus only takes into account a small sample of the total recorded neural activity. Next, we applied a more inclusive analysis, using all simultaneously recorded neural activity during individual sessions to determine whether odor identity could be decoded from the complete ensemble response on a single-trial basis. This analysis takes into account subtle variations in responses across conditions, and trials within conditions—variability that is lost in the single-neuron-based analyses presented above—and thus more closely mimics real-world conditions where animals need to identify an odor during a single encounter using the entire population of pPC responses. For each odor, we calculated an ensemble response profile consisting of a vector of firing rates (one for each simultaneously-recorded neuron, averaged across the stimulus period). Discriminability of odors A and B was calculated by comparing the distance between each single-trial ensemble response profile and each of two trial-averaged ensemble response templates (one for odor A; one for odor B). A trial was classified correctly if the distance between the trial and the matching template was smallest (i.e., when the distance between an odor A trial and the odor A template was smaller than the distance between the odor A trial and the odor B template, and vice versa). Figure 6A shows the average decoding performance over all sessions that featured at least 2 simultaneously recorded neurons (n=20 sessions both pre and post conditioning; mean number of neurons per ensemble [pre/post]: 6.3/6.7; range: 2-16/2-12). Overall, the pattern of results is consistent with the one obtained from single neurons (see Figure 5A): Early in the response, ensembles recorded both pre and post conditioning performed above chance. However, whereas decoding performance pre conditioning dropped during the late portion of the response, performance post conditioning remained high. This pattern was confirmed by ANOVA, revealing a Window × Epoch interaction ($F_{1,37}$=5.79, $p<0.05$). Next, we examined more closely the firing rate patterns on which decoding performance is based. Figure 6Bi shows decoding performance obtained from an example ensemble of 10 simultaneously recorded neurons post conditioning in a sliding window over time. The dynamics of the binned ensemble response during the stimulus period is shown in Figure 6Bii. Even though decoding performance was mostly above chance during the entire stimulus

period, response patterns underwent profound changes over the course of the response, such that neurons preferring odor A early in the response switch to preferring odor B later in the response, and *vice versa*. Such changes in selectivity are consistent with the results from the single neuron analysis presented above (see Figure 5B), suggesting that odor representations change over the course of the response. To directly test whether this is true at the ensemble level, we compared single-trial ensemble responses to the same odor between two time windows (one early in the response; one late in the response). In other words, we asked the question: How well can we decode odor identity from late epoch ensemble responses using templates obtained from the early epoch? Figure 6C shows the result of this analysis. Ensemble responses to odor B during early and late epochs were easily distinguished, indicating that responses to odor B differed between epochs. In contrast, ensemble responses to odor A were more similar between epochs (t-test comparing discriminability of early and late epoch responses between odors A and B: $t_{12}=2.46$, $p<0.05$). No differences were found in between-epoch discriminability of responses to the same odors pre conditioning—a pattern that differed significantly from the one observed post conditioning (t-test comparing the difference in discriminability between odors A and B pre versus post conditioning: $t_{19}=2.60$, $p<0.05$). Together, results from the decoding analysis demonstrate that odor identity can be read out early in the response using relatively small ensembles of pPC neurons, regardless of conditioning. Conditioning further enhances discriminability between conditioned and unconditioned odors in a manner that is selective to the late response epoch, and is characterized by a unique ensemble response code.

Ensemble decoding accuracy does not depend on palatability

The results presented above indicate that taste-odor association learning increases discriminability between the representations of odors A and B in the late portion of pPC ensemble responses. However, it is unclear what aspect of odors is reflected exactly in the response of pPC neurons. One possibility is that the late response epoch reflects odor palatability. Our behavioral results (Figure 2) show that the palatability of the saccharin-associated odor increases after conditioning, and this increase in palatability could therefore be driving changes in pPC ensemble response patterns. To directly test for this possibility, we

399 performed linear regression of ensemble discriminability during the late epoch on preference
400 for odor B (Figure 7A). This analysis yielded no significant effect of preference on odor
401 discriminability ($F=1.46$, $p=0.24$). Regression using pre versus post conditioning as a predictor
402 (Figure 7B) confirmed that discriminability increased following association learning ($F=5.70$,
403 $p<0.05$). Thus, these findings suggest that ensemble discriminability cannot be explained by
404 odor palatability, but instead reflects other aspects of odor perception.

405 **Discussion**

406 Our results demonstrate that taste-odor association learning changes responses of pPC neurons
407 to odor solutions. Association-related changes in responsiveness appeared as changes in the
408 dynamics of stimulus-evoked responses, leading to enhanced discriminability between
409 representations of taste-associated and non-taste-associated odors. Learning-related activity
410 patterns were selective to the late portion of the response, and qualitatively different from the
411 patterns observed during the early portion of the response. We speculate that during oral
412 evaluation of odor stimuli, association-related representations are generated by ongoing
413 interactions with the taste system and can be read-out by downstream brain areas
414 independently of chemical identity representations.

415 Experience-dependent coding of olfactory information is supported by the organization
416 of the primary olfactory (piriform) cortex. Information about odorant identity is relayed from
417 olfactory sensory neurons to the piriform cortex via the olfactory bulb, and is represented in
418 unique but partly overlapping ensembles of neurons that are distributed throughout the
419 piriform cortex without apparent spatial organization (Scott et al., 1980; Schwob and Price,
420 1984; Rennaker et al., 2007; Stettler and Axel, 2009; Miyamichi et al., 2011; Sosulski et al.,
421 2011). Besides bottom-up sensory input from the olfactory bulb, piriform cortex also receives
422 inputs from various extra-olfactory systems (Luskin and Price, 1983; Johnson et al., 2000;
423 Haberly, 2001; Majak et al., 2004; Sadrian and Wilson, 2015). Our findings are generally in line
424 with previous work demonstrating that experience can shape cortical odor representations
425 (Kadohisa and Wilson, 2006; Li et al., 2006; Calu et al., 2007; Roesch et al., 2007; Li et al., 2008;
426 Barnes et al., 2011; Chen et al., 2011; Chapuis and Wilson, 2012; Gire et al., 2013; Meissner-
427 Bernard et al., 2019; Wang et al., 2019), and shed new light on the mechanisms underlying
428 context-dependent cortical olfactory coding. One possible way of encoding experience is
429 through plasticity in the local cortical circuit. In this scenario, experience affects how bottom-up
430 inputs from the bulb are processed by the local cortical circuit, resulting in a static
431 rearrangement of odor relationships. For example, Chapuis et al. (Chapuis and Wilson, 2012)
432 showed that cortical representations of the components of an odor mixture may become more
433 or less similar to each other, depending on whether rats were rewarded to respond to the

mixture in a configural or elemental manner, respectively. In addition to experience-dependent changes in the local representation of bottom-up input patterns, some studies have suggested that piriform cortex may explicitly encode associative features of odor stimuli independently of chemical identity (Calu et al., 2007; Roesch et al., 2007; Gire et al., 2013; Meissner-Bernard et al., 2019; Wang et al., 2019). Conversely, others have suggested that explicit encoding of associative features occurs elsewhere in the brain (Millman and Murthy, 2020; Wang et al., 2020).

The present findings suggest that pPC neurons explicitly encode taste associations of odors in the temporal dynamics of their response, uncovering new insight into the mechanisms underlying context-dependent cortical odor coding. Experience-dependent changes did not appear as static changes in odor representations. That is, changes were not uniform across the response period. Instead, experience-dependent changes were confined to the late portion of the response. Changes in response dynamics following conditioning did not simply sustain the representation observed during the early portion of the response, but led to the emergence of a new representation. Taken together, these findings suggests that pPC neurons multiplex information using a dynamic coding scheme, where different aspects of an odor stimulus are represented during different epochs over the course of the response. With respect to the early response period (initial 1 s following stimulus delivery), we speculate—in line with previous work on piriform cortical odor coding—that activity patterns reflect bottom-up input from the olfactory bulb containing information about odor identity (Rennaker et al., 2007; Poo and Isaacson, 2009; Stettler and Axel, 2009; Bolding and Franks, 2017). With respect odor information that appeared selectively after conditioning during the late response period (after 1 second following stimulus deliver), activity patterns may encode taste associations of odors; alternatively, they may reflect hedonic value of odors. The former interpretation is consistent with the proposed role for piriform cortex in stimulus identity processing, and pPC neurons may dynamically represent chemical odor identity and associated taste identity. Indeed, behavioral work in humans suggests that taste associations of odors can be taste-specific (Stevenson et al., 1995; Stevenson et al., 1998; Stevenson et al., 2000a; Stevenson et al., 2000b; Stevenson and Boakes, 2004; Yeomans et al., 2006). Moreover, we did not find any evidence that the late

463 portion of the pPC response reflects odor palatability. Future work in which animals learn to
464 associate different odors with different tastes that vary in quality and hedonic value will more
465 explicitly characterize the nature of information encoded in the different response epochs.

466 Few studies to date have explicitly considered the temporal dynamics of cortical odor
467 responses and their relation to associative coding. One notable exception is a study by Gire et
468 al. (Gire et al., 2013), who recorded from neurons in the posterior piriform cortex of rats to
469 rewarded and unrewarded odors. They considered the contribution of activity patterns at two
470 temporal scales: inhalation-locked and non-inhalation-locked. Whereas information about
471 chemical identity was present in fast, inhalation-locked responses that are thought to reflect
472 processing of bottom-up inputs by local piriform cortical circuits (Bolding and Franks, 2018),
473 information about reward value was present in slower activity patterns that were not locked to
474 respiration. The slow dynamics of experience-dependent activity pattern observed in the
475 present study and by Gire et al. suggest that they are conveyed to pPC by top-down inputs.
476 Together, findings from both studies support a model in which associative odor coding emerges
477 dynamically through ongoing interactions with extra-olfactory systems. More broadly, a
478 dynamic model of odor coding in pPC is in line with previous observations of response dynamics
479 at time scales beyond the sniff cycle (Rennaker et al., 2007; Wang et al., 2019).

480 Dynamic multiplexing of sensory and associative information at timescales similar to the
481 ones observed in the present study has previously been observed in other brain regions that
482 process consumption-related sensory cues. For example, activity patterns in the insular
483 gustatory cortex reflect taste identity during the initial second following intra-oral taste
484 delivery; followed by activity patterns that reflect hedonic value of the taste stimulus,
485 independent of stimulus identity (Katz et al., 2001; Sadacca et al., 2012). Moreover, EMG
486 recordings of orofacial movements in response to intra-oral taste solutions demonstrate that
487 changes in GC neuron response patterns precede the expression of palatability-related
488 behavioral responses, suggesting a causal role for response dynamics in controlling behavior (Li
489 et al., 2016; Mukherjee et al., 2019). These response dynamics arise from ongoing interactions
490 with the basolateral amygdala (Fontanini et al., 2009; Piette et al., 2012; Lin et al., 2021). In the
491 present study, we did not measure behavioral responses on a trial-by-trial basis, but the

temporal scale of the observed dynamics is broadly consistent with a role in oral evaluation of sensory stimuli. Future work measuring orofacial movements (e.g., mouth movements, sniffing) in real time will determine the temporal relation between behavioral and neural response patterns.

The effects of conditioning observed in the present study constitute relatively subtle changes in neural response patterns. Odor responsiveness in individual neurons was overall sparse, and conditioning did not result in significant changes in responsiveness of individual neurons (i.e., we did not observe an increase or decrease in the number of neurons that responded significantly to odor stimuli). The lack of sensitivity in single neuron analysis may be due to a high degree of response variability. One factor that likely contributed to response variability across trials is the protracted nature of the response. Responses of single pPC neurons unfolded over seconds following stimulus delivery and are poorly locked to stimulus onset. Another source of variability is that neural activity appeared to change in a heterogenous manner, with some neurons increasing and others decreasing their activity levels in a dynamic manner. These issues underscore the value of ensemble analysis that takes into account correlated, heterogeneous changes in neural activity across multiple neurons on a single trial basis. Indeed, our ensemble decoding analysis was able to significantly discriminate between odor representations using responses from relatively small ensembles of pPC neurons.

The changes in pPC responsiveness following taste association learning observed here are reminiscent of the changes in pPC responses to odor solutions when presented in mixture with taste compounds. We recently demonstrated that taste and odor components of mixtures interact to change responses of pPC neurons in real time (Idris et al., 2023). Multisensory modulations observed in that study resembled the experience-dependent modulations observed here in that they were mostly subtle at the single neuron level, heterogenous in nature, and led to greater discriminability of odor representations at the ensemble level. Also in line with the present findings, increased discriminability resulting from real-time multisensory modulation was not observed until later in the response, following an initial unisensory odor-selective phase. The fact that we recorded from separate populations of neurons before and after conditioning precludes a direct comparisons between real-time and experience-driven

pPC response modulation, future work aimed at tracking the activity of single neurons across conditioning will determine whether real-time interactions between taste and smell components of mixture are predictive of experience-dependent modulations.

Regarding potential extra-olfactory sources relaying associative input about taste, previous work has identified GC as a candidate region, as inactivation of GC prohibited the expression of preferences for sweet taste-associated odors (Maier et al., 2015; Blankenship et al., 2019). Based on previous findings, the influence of GC on olfactory processing appears to be specific to the context of consumption. Intra-oral delivery of odors in solution creates a unique context that has been shown to play a key role in mediating taste-odor association learning. Blankenship et al. (Blankenship et al., 2019) demonstrated that animals more readily learn preferences for sweet taste-associated odor when odors were presented intra-orally versus ortho-nasally, and that inactivating GC selectively affected the expression of preferences for intra-orally presented sweet taste-associated odors. Further evidence for unique processing of consumption-related odor signals comes from human imaging work, showing increased BOLD signal in GC in response to food odors versus non-food odors (Veldhuizen et al., 2010). Although it remains unclear whether the response patterns observed in the present study are unique to the context of consumption, pPC neurons have been shown to be sensitive to oral context: responses to the same odorant presented intra-orally and ortho-nasally can differ substantially (Maier, 2017). Together, these findings suggest that oral context may play a key role in generating the response patterns observed in the present study.

Figure Captions

Figure 1. Histological reconstruction of recording sites. A. Schematic from a rat brain atlas (Paxinos and Watson, 1986) indicating the general region of the posterior piriform cortex layers I, II and III in a coronal view (1.4 mm posterior to bregma). **B-C.** Coronal sections taken from two rat brains showing DAPI (blue) and DiI (pink) staining of nuclei and electrode tracts, respectively. Scalebar indicates 0.75 mm. Electrode tips are indicated by arrowheads. Animal in B was implanted with a microwire array; animal in C with a silicon probe.

Figure 2. Odor-taste association paradigm. A. Sequence of procedures in the experimental paradigm. **B.** Preferences for the saccharin-paired odor (odor B) obtained before and after conditioning for each animal (gray lines). Averages (±SEM) over animals (n=29) are shown in color. **C.** Change in preference (post–pre conditioning), averaged (±SEM) over animals.

Figure 3. Responses to intra-oral odor solutions recorded from exemplar pPC neurons. A-D. Top panels show 100 randomly selected waveforms (grey) in the single neuron cluster; middle panels are spike raster plots showing all action potentials for all trials aligned on stimulus delivery (t=0); and bottom panels show average firing rate (±SEM) over trials in response to odors A and B. Rate plots are calculated using a 500 ms sliding window to illustrate the temporal profile of responses, but lack the temporal resolution of raster plots due to the size of the smoothing window. Neurons in A and B were recorded before conditioning; neurons in C and D after conditioning. Dashed lines indicate offset of "early" and "late" response epochs.

Figure 4. Odor responsiveness in the population of pPC neurons. A-B. Proportion of pPC neurons exhibiting a significant response relative to baseline, before (A) and after (B) conditioning. Responsiveness was calculated using a 500 ms sliding window. Dashed lines indicate offset of "early" and "late" response epochs. No significant differences in responsiveness were observed (X^2 test comparing proportions between groups).

Figure 5. Discriminability between odors A and B at the single neuron level. A. Effect size (Cohen's d) of the difference in the response to odors A and B, averaged (±SEM) over all neurons recorded before and after conditioning (n=152 and 147, respectively), during baseline, and early and late stimulus response epochs. **B.** Cohen's d obtained from the early and late

response epochs for all odor-responsive neuron (n=36 before and after conditioning). Letters correspond to the example responses in Figure 3.

Figure 6. Single-trial decoding of odor identity from ensemble responses. A. Discriminability between odors A and B, averaged (±SEM) over all sessions with n>1 neurons before and after conditioning (n=20), during baseline, and early and late stimulus response epochs. **Bi.** Discriminability as a function of time for an example ensemble recorded after conditioning (n=10 neurons). Stimulus period (2500 ms following stimulus onset) is highlighted. **Bii.** Firing rate patterns for all neurons in the example ensemble shown in Bi. Responses are shown in a series of sliding windows (500 ms window size, 100 ms step size). **C.** Discriminability of ensemble responses to the same odor in different response epochs. *t-test: $p<0.05$.

Figure 7. Relation between ensemble decoding accuracy and odor palatability. A. Ensemble discriminability between odors A and B during the late response epoch as a function of relative preference for odor B for each animal (n=19). No significant relation was detected by linear regression. **B.** Ensemble discriminability between odors A and B during the late response epoch before and after conditioning for each animal (n=19). *Regression: $p<0.05$.

References

Avery JA, Liu AG, Ingeholm JE, Riddell CD, Gotts SJ, Martin A (2020) Taste quality representation in the human brain. J Neurosci 40:1042-1052.

Barnes DC, Chapuis J, Chaudhury D, Wilson DA (2011) Odor fear conditioning modifies piriform cortex local field potentials both during conditioning and during post-conditioning sleep. PLoS One 6:e18130.

Blankenship ML, Grigorova M, Katz DB, Maier JX (2019) Retronasal odor perception requires taste cortex, but orthonasal does not. Curr Biol 29:62-69.e63.

Bolding KA, Franks KM (2017) Complementary codes for odor identity and intensity in olfactory cortex. Elife 6.

Bolding KA, Franks KM (2018) Recurrent cortical circuits implement concentration-invariant odor coding. Science 361.

Bushdid C, Magnasco MO, Vosshall LB, Keller A (2014) Humans can discriminate more than 1 trillion olfactory stimuli. Science 343:1370-1372.

Calu DJ, Roesch MR, Stalnaker TA, Schoenbaum G (2007) Associative encoding in posterior piriform cortex during odor discrimination and reversal learning. Cereb Cortex 17:1342-1349.

Chapuis J, Wilson DA (2012) Bidirectional plasticity of cortical pattern recognition and behavioral sensory acuity. Nat Neurosci 15:155-161.

Chen CF, Barnes DC, Wilson DA (2011) Generalized vs. stimulus-specific learned fear differentially modifies stimulus encoding in primary sensory cortex of awake rats. J Neurophysiol 106:3136-3144.

Christensen BA, Triplett CS, Maier JX (2022) Odor mixture perception during flavor consumption in rats. Behav Neurosci 136:300-306.

Elliott VE, Maier JX (2020) Multisensory interactions underlying flavor consumption in rats: the role of experience and unisensory component liking. Chem Senses 45:27-35.

Fontanini A, Grossman SE, Figueroa JA, Katz DB (2009) Distinct subtypes of basolateral amygdala taste neurons reflect palatability and reward. J Neurosci 29:2486-2495.

Gadziola MA, Tylicki KA, Christian DL, Wesson DW (2015) The olfactory tubercle encodes odor valence in behaving mice. J Neurosci 35:4515-4527.

Gautam SH, Verhagen JV (2012) Direct behavioral evidence for retronasal olfaction in rats. PLoS One 7:e44781.

Gire DH, Whitesell JD, Doucette W, Restrepo D (2013) Information for decision-making and stimulus identification is multiplexed in sensory cortex. Nat Neurosci 16:991-993.

Haberly LB (2001) Parallel-distributed processing in olfactory cortex: new insights from morphological and physiological analysis of neuronal circuitry. Chem Senses 26:551-576.

Holman E (1975) Immediate and delayed reinforcers for flavor preferences in rats. Learn Motiv 6:91-100.

Idris A, Christensen BA, Walker EM, Maier JX (2023) Multisensory integration of orally-sourced gustatory and olfactory inputs to the posterior piriform cortex in awake rats. J Physiol 601:151-169.

Johnson DM, Illig KR, Behan M, Haberly LB (2000) New features of connectivity in piriform cortex visualized by intracellular injection of pyramidal cells suggest that "primary" olfactory cortex functions like "association" cortex in other sensory systems. J Neurosci 20:6974-6982.

Kadohisa M, Wilson DA (2006) Separate encoding of identity and similarity of complex familiar odors in piriform cortex. Proc Natl Acad Sci U S A 103:15206-15211.

Karunanayaka PR, Wilson DA, Vasavada M, Wang J, Martinez B, Tobia MJ, Kong L, Eslinger P, Yang QX (2015) Rapidly acquired multisensory association in the olfactory cortex. Brain Behav 5:e00390.

Katz DB, Simon SA, Nicolelis MA (2001) Dynamic and multimodal responses of gustatory cortical neurons in awake rats. J Neurosci 21:4478-4489.

632 Li JX, Maier JX, Reid EE, Katz DB (2016) Sensory Cortical Activity Is Related to the Selection of a Rhythmic
633 Motor Action Pattern. J Neurosci 36:5596-5607.
634 Li W, Luxenberg E, Parrish T, Gottfried JA (2006) Learning to smell the roses: experience-dependent
635 neural plasticity in human piriform and orbitofrontal cortices. Neuron 52:1097-1108.
636 Li W, Howard JD, Parrish TB, Gottfried JA (2008) Aversive learning enhances perceptual and cortical
637 discrimination of indiscriminable odor cues. Science 319:1842-1845.
638 Lin JY, Mukherjee N, Bernstein MJ, Katz DB (2021) Perturbation of amygdala-cortical projections reduces
639 ensemble coherence of palatability coding in gustatory cortex. Elife 10.
640 Luskin MB, Price JL (1983) The topographic organization of associational fibers of the olfactory system in
641 the rat, including centrifugal fibers to the olfactory bulb. J Comp Neurol 216:264-291.
642 Maier JX (2017) Single-neuron responses to intraoral delivery of odor solutions in primary olfactory and
643 gustatory cortex. J Neurophysiol 117:1293-1304.
644 Maier JX, Elliott VE (2020) Adaptive weighting of taste and odor cues during flavor choice. J
645 Neurophysiol.
646 Maier JX, Blankenship ML, Li JX, Katz DB (2015) A multisensory network for olfactory processing. Curr
647 Biol 25:2642-2650.
648 Majak K, Rönkkö S, Kemppainen S, Pitkänen A (2004) Projections from the amygdaloid complex to the
649 piriform cortex: A PHA-L study in the rat. J Comp Neurol 476:414-428.
650 McQueen KA, Fredericksen KE, Samuelsen CL (2020) Experience informs consummatory choices for
651 congruent and incongruent odor-taste mixtures in rats. Chem Senses 45:371-382.
652 Meissner-Bernard C, Dembitskaya Y, Venance L, Fleischmann A (2019) Encoding of Odor Fear Memories
653 in the Mouse Olfactory Cortex. Curr Biol 29:367-380.e364.
654 Millman DJ, Murthy VN (2020) Rapid Learning of Odor-Value Association in the Olfactory Striatum. J
655 Neurosci 40:4335-4347.
656 Miyamichi K, Amat F, Moussavi F, Wang C, Wickersham I, Wall NR, Taniguchi H, Tasic B, Huang ZJ, He Z,
657 Callaway EM, Horowitz MA, Luo L (2011) Cortical representations of olfactory input by trans-
658 synaptic tracing. Nature 472:191-196.
659 Mukherjee N, Wachutka J, Katz DB (2019) Impact of precisely-timed inhibition of gustatory cortex on
660 taste behavior depends on single-trial ensemble dynamics. Elife 8.
661 Paxinos G, Watson C (1986) The rat brain atlas: Academic Press, Inc., San Diego, Calif.
662 Phillips MI, Norgren RE (1970) A Rapid Method for Permanent Implantation of an Intraoral Fistula in
663 Rats. Behavior Research Methods & Instrumentation 2:124-&.
664 Piette CE, Baez-Santiago MA, Reid EE, Katz DB, Moran A (2012) Inactivation of basolateral amygdala
665 specifically eliminates palatability-related information in cortical sensory responses. Journal of
666 Neuroscience 32:9981-9991.
667 Poo C, Isaacson JS (2009) Odor representations in olfactory cortex: "sparse" coding, global inhibition,
668 and oscillations. Neuron 62:850-861.
669 Quiroga RQ, Reddy L, Koch C, Fried I (2007) Decoding visual inputs from multiple neurons in the human
670 temporal lobe. J Neurophysiol 98:1997-2007.
671 Rennaker RL, Chen CF, Ruyle AM, Sloan AM, Wilson DA (2007) Spatial and temporal distribution of
672 odorant-evoked activity in the piriform cortex. J Neurosci 27:1534-1542.
673 Roesch MR, Stalnaker TA, Schoenbaum G (2007) Associative encoding in anterior piriform cortex versus
674 orbitofrontal cortex during odor discrimination and reversal learning. Cereb Cortex 17:643-652.
675 Rossant C, Kadir SN, Goodman DFM, Schulman J, Hunter MLD, Saleem AB, Grosmark A, Belluscio M,
676 Denfield GH, Ecker AS, Tolias AS, Solomon S, Buzsaki G, Carandini M, Harris KD (2016) Spike
677 sorting for large, dense electrode arrays. Nat Neurosci 19:634-641.
678 Sadacca BF, Rothwax JT, Katz DB (2012) Sodium concentration coding gives way to evaluative coding in
679 cortex and amygdala. Journal of Neuroscience 32:9999-10011.

680 Sadrian B, Wilson DA (2015) Optogenetic Stimulation of Lateral Amygdala Input to Posterior Piriform
681 Cortex Modulates Single-Unit and Ensemble Odor Processing. Front Neural Circuits 9:81.
682 Schwob JE, Price JL (1984) The development of axonal connections in the central olfactory system of
683 rats. J Comp Neurol 223:177-202.
684 Sclafani A, Ackroff K (1994) Glucose- and fructose-conditioned flavor preferences in rats: taste versus
685 postingestive conditioning. Physiol Behav 56:399-405.
686 Scott JW, McBride RL, Schneider SP (1980) The organization of projections from the olfactory bulb to the
687 piriform cortex and olfactory tubercle in the rat. J Comp Neurol 194:519-534.
688 Slotnick BM, Westbrook F, Darling FMC (1997) What the rat's nose tells the rat's mouth: Long delay
689 aversion conditioning with aqueous odors and potentiation of taste by odors. Animal Learning
690 and Behavior 25:357-369.
691 Sosulski DL, Bloom ML, Cutforth T, Axel R, Datta SR (2011) Distinct representations of olfactory
692 information in different cortical centres. Nature 472:213-216.
693 Stettler DD, Axel R (2009) Representations of odor in the piriform cortex. Neuron 63:854-864.
694 Stevenson R, Boakes R (2004) Sweet and sour smells: learned synaesthesia between the senses of taste
695 and smell. In: The handbook of multisensory processing (Calvert G, Spence C, Stein B, eds), pp
696 69-83. Cambridge, MA: MIT Press.
697 Stevenson R, Prescott J, Boakes R (1995) The acquisition of taste properties by odors. Learning and
698 Motivation 26:433-455.
699 Stevenson RJ, Boakes RA, Prescott J (1998) Changes in odor sweetness resulting from implicit learning of
700 a simultaneous odor-sweetness association: an example of learned synesthesia. Learning and
701 Motivation 29:113-132.
702 Stevenson RJ, Boakes RA, Wilson JP (2000a) Counter-conditioning following human odor–taste and
703 color–taste learning. Learning and Motivation 31:114-127.
704 Stevenson RJ, Boakes RA, Wilson JP (2000b) Resistance to extinction of conditioned odor perceptions:
705 evaluative conditioning is not unique. J Exp Psychol Learn Mem Cogn 26:423-440.
706 Veldhuizen MG, Nachtigal D, Teulings L, Gitelman DR, Small DM (2010) The insular taste cortex
707 contributes to odor quality coding. Front Hum Neurosci 4.
708 Wang D, Liu P, Mao X, Zhou Z, Cao T, Xu J, Sun C, Li A (2019) Task-Demand-Dependent Neural
709 Representation of Odor Information in the Olfactory Bulb and Posterior Piriform Cortex. J
710 Neurosci 39:10002-10018.
711 Wang PY, Boboila C, Chin M, Higashi-Howard A, Shamash P, Wu Z, Stein NP, Abbott LF, Axel R (2020)
712 Transient and Persistent Representations of Odor Value in Prefrontal Cortex. Neuron 108:209-
713 224.e206.
714 Wilson DA, Stevenson RJ (2003) The fundamental role of memory in olfactory perception. Trends
715 Neurosci 26:243-247.
716 Wilson DA, Best AR, Sullivan RM (2004) Plasticity in the olfactory system: lessons for the neurobiology of
717 memory. Neuroscientist 10:513-524.
718 Yeomans MR, Mobini S, Elliman TD, Walker HC, Stevenson RJ (2006) Hedonic and sensory characteristics
719 of odors conditioned by pairing with tastants in humans. J Exp Psychol Anim Behav Process
720 32:215-228.
721 Zelano C, Bensafi M, Porter J, Mainland J, Johnson B, Bremner E, Telles C, Khan R, Sobel N (2005)
722 Attentional modulation in human primary olfactory cortex. Nat Neurosci 8:114-120.

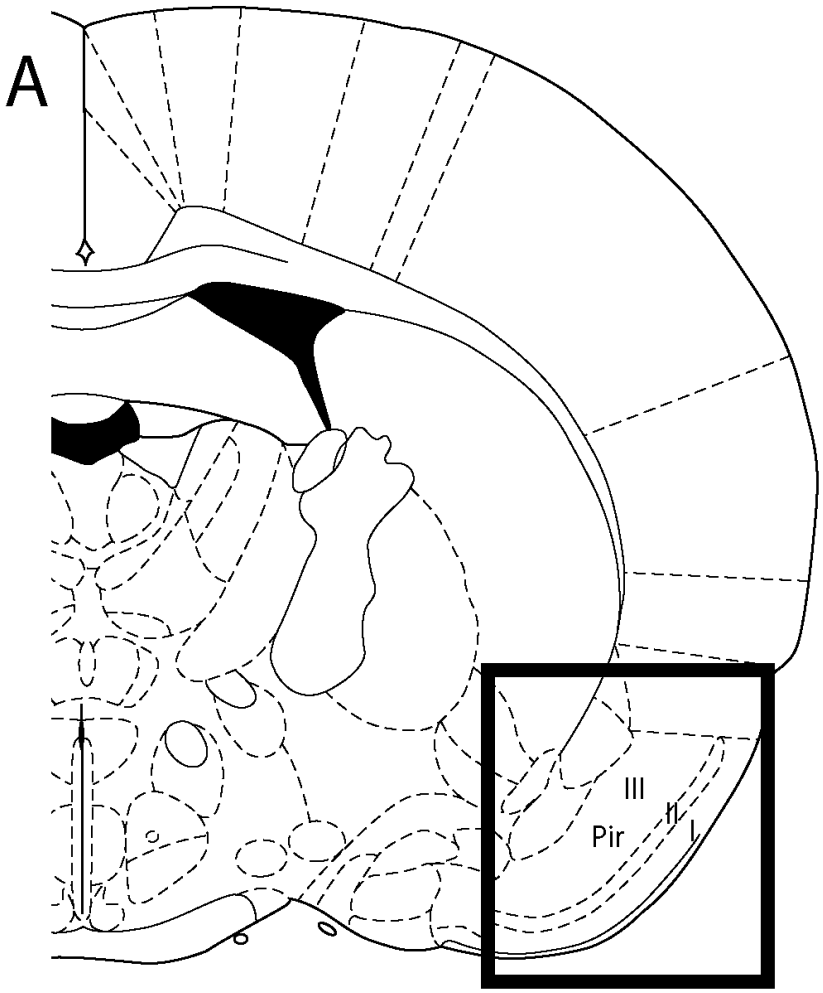

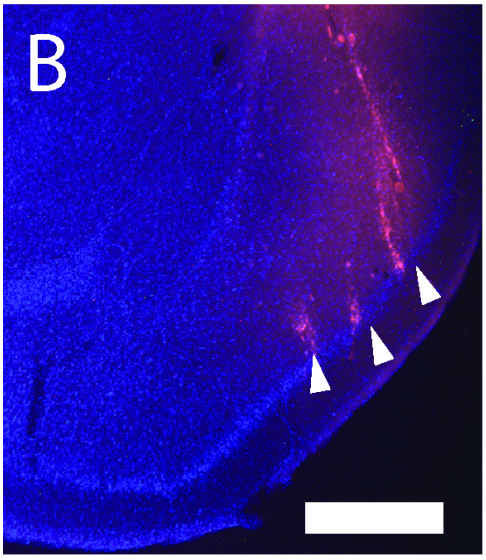

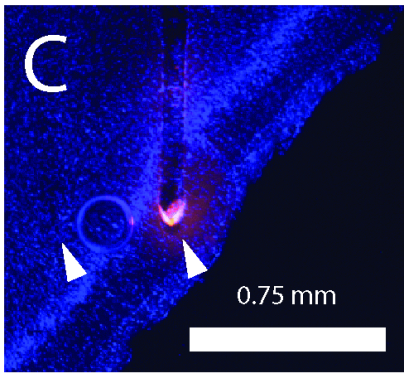

A

Day		Procedure
1	*Daytime*	**Pre Recording**
	Nighttime	**Pre Preference Test**
2	*Daytime*	
	Nighttime	
3	*Daytime*	**Train 1**
	Nighttime	
4	*Daytime*	**Train 2**
	Nighttime	
5	*Daytime*	**Train 3**
	Nighttime	
6	*Daytime*	**Train 4**
	Nighttime	
7	*Daytime*	**Post Recording**
	Nighttime	**Post Preference Test**

B

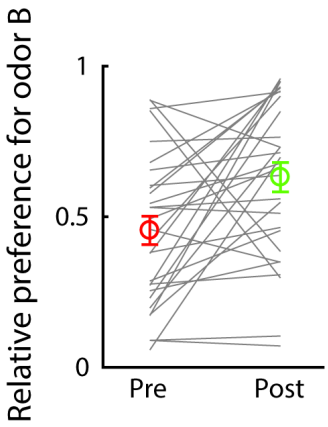

C